Detecting ultrafast interatomic electronic processes in media by fluorescence

2014 New J. Phys. 16 102002

(http://iopscience.iop.org/1367-2630/16/10/102002)

New Journal of Physics
The open access journal at the forefront of physics
Deutsche Physikalische Gesellschaft DPG | IOP Institute of Physics

Fast Track Communication

Detecting ultrafast interatomic electronic processes in media by fluorescence

André Knie[1], Andreas Hans[1], Marko Förstel[2], Uwe Hergenhahn[2], Philipp Schmidt[1], Philipp Reiß[1], Christian Ozga[1], Benjamin Kambs[1], Florian Trinter[3], Jörg Voigtsberger[3], Daniel Metz[3], Till Jahnke[3], Reinhard Dörner[3], Alexander I Kuleff[4], Lorenz S Cederbaum[4], Philipp V Demekhin[1] and Arno Ehresmann[1]

[1] Institut für Physik, Universität Kassel, Heinrich-Plett-Str. 40, D-34132 Kassel, Germany
[2] Max-Planck-Institut für Plasmaphysik, EURATOM Association, Wendelsteinstr. 1, D-17491 Greifswald, Germany
[3] Institut für Kernphysik, J W Goethe Universität, Max-von-Laue-Str. 1, D-60438 Frankfurt, Germany
[4] Theoretische Chemie, Physikalisch-Chemisches Institut, Universität Heidelberg, Im Neuenheimer Feld 229, D-69120 Heidelberg, Germany
E-mail: knie@physik.uni-kassel.de and ehresmann@physik.uni-kassel.de

Received 10 July 2014, revised 22 August 2014
Accepted for publication 19 September 2014
Published 9 October 2014

New Journal of Physics **16** (2014) 102002

doi:10.1088/1367-2630/16/10/102002

Abstract

Interatomic coulombic decay (ICD), a radiationless transition in weakly bonded systems, such as solutes or van der Waals bound aggregates, is an effective source for electrons of low kinetic energy. So far, the ICD processes could only be probed in ultra-high vacuum by using electron and/or ion spectroscopy. Here we show that resonant ICD processes can also be detected by measuring the subsequently emitted characteristic fluorescence radiation, which makes their study in dense media possible.

Keywords: cluster, fluorescence, ICD

1. Introduction

Interatomic coulombic decay (ICD) is a recently discovered mechanism responsible for ultrafast transfer of electronic excitation energy [1] and for production of low kinetic energy electrons [2–4] that can have profound implications in radiation chemistry [5] and for radiation initiated processes in biochemistry [6]. Experiments on ICD so far relied on the detection of charged particles (electrons, ions) emitted from clusters or from a liquid jet in an ultra-high vacuum [7]. These techniques cannot easily be extended to systems of biological relevance in their natural environment, as the necessary vacuum conditions cannot be met and as the characteristic electrons and ion pairs cannot be detected inside a medium. Here we show that ICD is observable by detecting subsequently emitted photons, a method also applicable to dense media. In a proof of concept experiment, characteristic fluorescence for resonant ICD after inner-valence excitation of Ne-clusters was unequivocally observed.

ICD as a strong source of low-energy electrons and ions was experimentally proven for the first time in neon clusters, by direct detection of the ICD electrons under ultra-high vacuum conditions [8, 9]. Follow-up investigations were performed on a variety of systems and using different set-ups, but experimentally stringent vacuum conditions of the sample environment were always required [7, 10]. For a quantification of electron emission by ICD in aqueous or soft-matter samples in an *in situ* environment these probes are not suitable, because the mean free path of electrons inside these dense media is too short [11]. *In situ* detection is even more desirable as a very recent theoretical prediction [12] and follow up experiments [13–15] show that a variant of the ICD process initiated by resonant excitation may enable the control of emission sites for low-energy electrons on an atomic level, allowing to directly address specific sites in marked cells [12], promising a new route for cancer therapy by x-rays. A dramatic enhancement of genotoxic low-energy electrons by ICD has also be recently seen for fast ion [16, 17] and electron [17] impact, showing that ICD is triggered by all forms of radiation used today in cancer therapy. Also for these projectiles *in situ* spectroscopy of ICD is of decisive interest.

Contrary to charged particles, photons can probe deeply inside dense media. Although photons might also be absorbed in tissue, their penetration depth is larger by orders of magnitude compared to low-energy charged particles. Measurements of emitted photons provide information about the emitter (site selectivity), its transition initial and final states (state selectivity), and on the lifetime of the emission process (time resolution). The photon-induced fluorescence spectroscopy [18] (PIFS) has been successfully used for the quantitative investigation of photoionization, Auger-, and autoionization processes in molecules [19–26] with particular sensitivity to processes with low-energy electron emission [19–21]. Despite the advantages mentioned above, fluorescence subsequent to ICD processes has not yet been recorded, as the target density in the necessary cluster experiments was very low. Advanced single photon counting techniques are, therefore, required to compensate for the expected small photon rates and to measure ICD.

Here, we report the first unambiguous proof of ICD by detection of fluorescence. Particularly amenable for our purposes are rare-gas clusters, since their generation can be controlled in a wide range of different sizes [27], from a few up to millions of atoms, allowing one to carry out experiments on well-defined samples. The present experiments were performed for the prototype Ne-clusters, for which it is known that resonant excitation of an inner valence electron triggers ICD [28–30]. The process is sketched in figure 1. An incoming photon

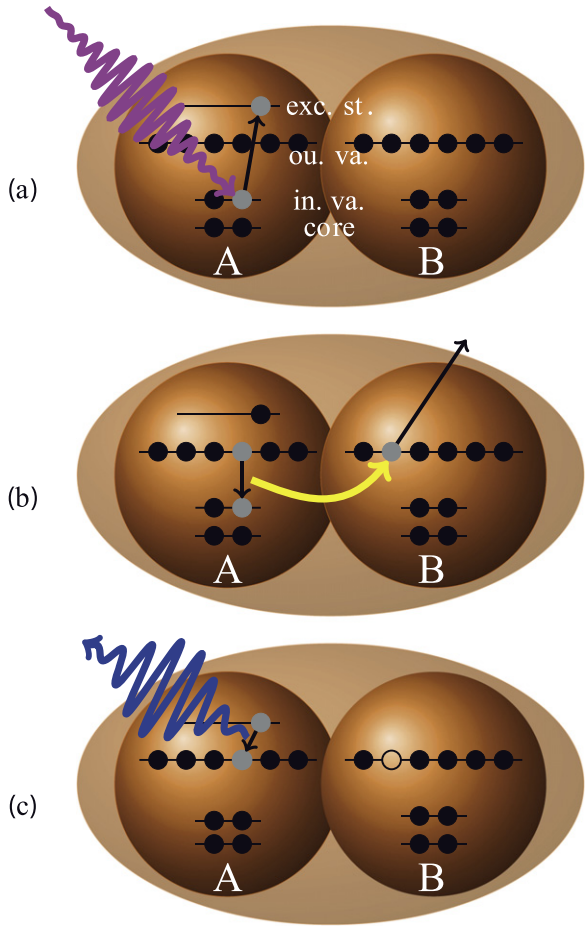

Figure 1. Schematic of fluorescence following ICD after resonant excitation in Ne-clusters. In the first step (a), an inner valence electron of atom A is resonantly excited. For an isolated atom or molecule, this excitation would result in fast relaxation of site A via its autoionization, which totally suppresses possible radiation emission. In the cluster, due to environment the energy can be alternatively transferred to a neighbour B via ICD, which results in the emission of a low-energy electron (b). The efficiency of ICD grows with the size of the cluster [31, 32] and may even dominate over autoionization on site A. Finally (c), the still excited atom A releases its energy by emission of a photon, which now becomes possible owing to the preceding ICD. Please note that, despite the atomic picture, the (outer) energy levels in the cluster might have changed dramatically, therefore, no atomic state notation is used in the figure.

resonantly excites an inner-valence (2s) electron of atom A (figure 1(a)). This electronic excitation is known to relax via two competing pathways: (i) by autoionization of the same atom A leading to the emission of fast electrons (kinetic energy between 23 and 27 eV); and, alternatively, (ii) via the resonant ICD which gives rise to the emission of slow electrons (kinetic energy between 0 and 10 eV) from atom B (figure 1(b)). Both processes are ultrafast and completely suppress the resonant fluorescence of the initially excited state. If the first pathway takes place, the relaxation process ends. This is not the case in the second pathway which is described in figure 1. Importantly, ICD becomes the dominant relaxation pathway when the cluster size grows [31, 32]. In ICD, a valence electron of atom A fills the hole in the

inner-valence shell. The energy gained is ultrafast transferred to a valence electron of a neighbouring atom B, leading to its release (figure 1(b)). As can be seen in figure 1, due to the presence of the excited electron, a part of the excess energy is still stored in atom A where one electron remains excited. This excess energy is not sufficient to further ionize the system and is released by the emission of a photon (figure 1(c)), which is used here to identify the preceding ICD.

2. Methods

In the present experiment a supersonic jet of Ne atoms and clusters was crossed with a linear polarized photon beam of monochromatized synchrotron radiation provided by the UE112-PGM1 beamline of the Helmholtz-Zentrum Berlin. The synchrotron was operating in single-bunch mode with a 800 ns bunch repetition of a single >1 ns (FWHM) wide bunch. A slit-width of 300 μm of the PGM was chosen to obtain a bandwidth of the synchrotron radiation of 26 meV at 48 eV. Parallel to the plane of polarization the cluster jet was produced by supersonic expansion through a nozzle into the experimental vacuum chamber. A conical copper nozzle with 80 μm diameter, 1.1 mm length, half opening angle of 15° was used. The nozzle was cooled by a liquid He flow and the temperature was stabilized to ±0.5 K. The degree of condensation, i.e., the ratio of monomers to clusters, was about 50%. The mean cluster size of $\langle N \rangle = 20$ was chosen large enough to enable detectable photon rates with the present advanced single-photon counting technique PIFS [18]. It was controlled following the formula of [27] with the present stagnation pressure of 518 mbar and nozzle temperature of 60 K.

The photons were collected by an open-face multi-channel plate detector, enabling single-photon counting and time resolved measurements. The detector was sensitive in a wavelength range between 40 and 120 nm, and no further wavelength selection within this interval was attempted. Since this is the first measurement of this kind, we would like to remove any doubt and simultaneously crosscheck our fluorescence measurements by additionally observing low-energy ICD electrons, a traditional direct proof of ICD. The cluster size was small allowing also for an easy detection of these electrons. The ICD-electrons were measured by a magnetic-bottle spectrometer described in [33] which was mounted perpendicular to the plane of polarization of the synchrotron radiation. A guiding field of 0.6 mT was used together with a 6 V acceleration voltage for the detection of these low-energy electrons.

3. Results

The total electron and fluorescence yields measured for the Ne-clusters as a function of exciting photon energy below the atomic 2s ionization threshold are shown in figure 2 by squares. Since the jet also contains uncondensed Ne atoms, the same yields recorded for a purely atomic beam are also depicted for comparison (circles). In the electron yield from the monomers (figure 2(a)), the well-known 2s-np autoionising atomic Rydberg resonances [34] are clearly visible. The corresponding fluorescence yield (figure 2(b)) does not exhibit prominent features and only at the energy close to the 2s-electron ionization threshold one observes a clear increase in intensity [35]. This is known to be due to fast autoionization of the 2s-np resonances, suppressing fluorescence emission, except for high-lying Rydberg states [36]. For the mixed cluster+atom jet, two additional peaks are seen in the 46.8–47.7 eV region of the total electron yield

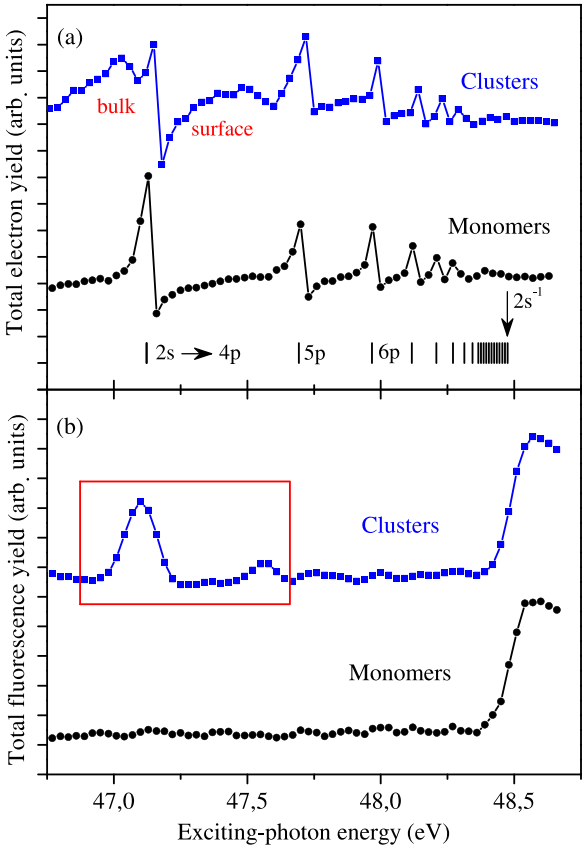

Figure 2. Total fluorescence and electron yields below the 2s ionization threshold of neon atoms and clusters. In panel (a), the total electron yield recorded for atoms (circles) is compared with that measured for clusters (squares). In panel (b), the corresponding total fluorescence yields are shown for atoms (circles) and for clusters (squares). The most prominent features in the electron yields of monomers and clusters are the autoionising 2s-np resonances, which produce high-energy (fast) electrons. These excitations do not lead to any fluorescence emission. The only prominent feature in the fluorescence yield of monomers starts at the ionization threshold of the 2s electron, above which subsequent radiative decay can take place. It is also seen for the cluster and atom mixture. In addition, two new features are visible in the electron and fluorescence yields of clusters. These were assigned to be the bulk and surface resonant excitation of the 2s-electron [29]. The two excitations may relax by ICD with subsequent emission of fluorescence, as drawn in figure 1. The resonant excitation region of interest (indicated by a rectangle) is shown in figure 3 on an enlarged scale.

(figure 2(a)) superposing the structure from the autoionising resonances. These two features are clearly visible in the fluorescence yield of the clusters (figure 2(b)), but not in the yield of the atoms.

In order to interpret these two features, we compare the fluorescence yield in figure 3 on an enlarged scale with the yield of low kinetic energy electrons recorded simultaneously. The enhancements in the low-energy electron yield (figure 3(a)), already observed at this photon energy earlier [28, 29], correspond to the bulk and surface resonances of the excited Ne-clusters [29] and have been identified to be due to ICD [28, 29]. The measured fluorescence yield (figure 3(b)) perfectly reproduces the structure of the ICD-electron spectrum. Therefore, these

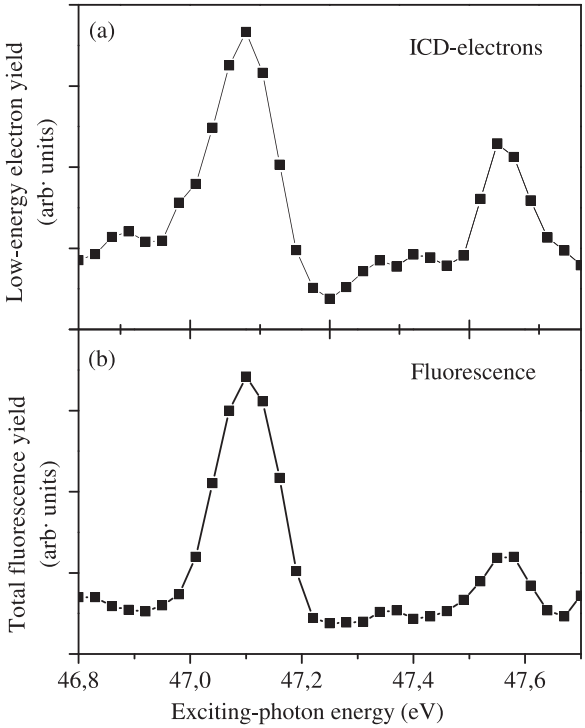

Figure 3. Fluorescence and low-energy electron yields in the resonant excitation region of neon clusters. The shown narrow energy range is indicated in figure 2(b) by a rectangle. In panel (a), the low-energy electron yield is shown, i.e., only electrons with kinetic energy between 0 and 10 eV emitted by the ICD are summed. Two distinct features are visible which were found to be the bulk and surface resonant excitation of the 2s-electron in neon clusters [29]. In panel (b), the respective fluorescence yield is shown. The direct correspondence between the two signals proves unambiguously that the observed fluorescence indeed evidences ICD. In dense media, fluorescence can be the only suitable probe to trace ICD, since low-energy electrons may not be able to escape.

new features in the fluorescence yield can be unequivocally interpreted as arising from ICD. More precisely, they are due to the radiative decay of the final states of the ICD process as indicated in figure 1(c). Contrary to the ICD electrons, this fluorescence can still be detected in dense media.

Being site and state selective [18–26], dispersed fluorescence provides extensive information on the emitter and on the initial and final states of the emission process. These advantages are routinely utilized in, e.g., astrophysics to characterize emission lines in small system [37]. Such a fluorescence-marker tool would be extremely desirable for biologically relevant systems and their constituent parts. For this, extensive characterization experiments supported by contemporary theoretical simulations on fluorescence in different emitters will be required. As cluster beams do usually consist of clusters and monomers, it is difficult to disentangle fluorescence from atoms and clusters when superimposed at a given wavelength. The present time-resolved PIFS experiment delivered a method to distinguish between fluorescence originating from atoms from that originating from clusters: fluorescence from atoms is emitted faster as the one from clusters. In our case, the 2s-ionization of Ne-atoms

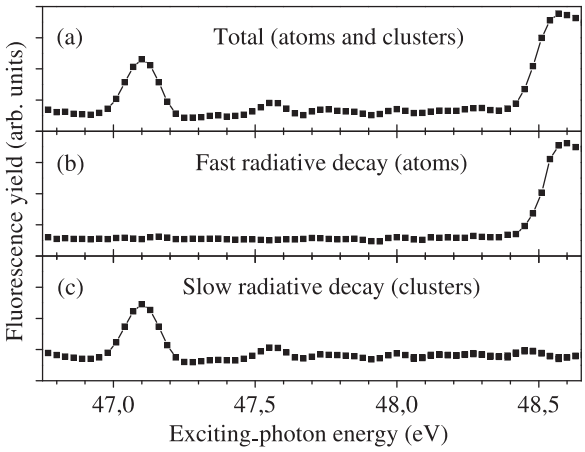

Figure 4. Time-resolved fluorescence yield for different intervals after the exciting synchrotron radiation pulse. The total time-integrated fluorescence signal (a) contains both features, the ICD signal originating from clusters and the threshold signal visible due to the sizeable admixture of atoms. The latter signal can be discriminated when only the fluorescent photons corresponding to the fast radiative decay in singly ionized atoms are measured (b). These were recorded at time delays, which are no longer than 2 ns after the exciting-pulse maximum. The yield of fluorescent photons, collected with time delays longer than 2 ns from the exciting-pulse maximum, is also presented (c). This fluorescence exhibits only the signals resulting from the slow radiative decay in the clusters subsequent to ICD.

results in a fast 2s-2p radiative decay with a lifetime of about 0.14 ns [36]. ICD occurs on the femtosecond time scale [1, 32, 38–41], orders of magnitude faster than the fluorescence emission. But the subsequent radiative decay in the clusters (figure 1(c)) is very slow and takes place on a 100 ns to 1 s time-scale (it is even dipole-forbidden in monomers). These two very different time-scales can be used to discriminate between the two signals observed in the total fluorescence yield (figure 4(a)). Figure 4(b) depicts fluorescence recorded from a mixed atom and cluster beam emitted earlier than 2 ns after the excitation pulse. This signal is identical to the fluorescence recorded for a pure atomic beam (figure 2(b)). Figure 4(c) depicts fluorescence emitted later than 2 ns from the excitation pulse, which contains the signal from the clusters without noticeable atomic fluorescence.

4. Conclusion

In conclusion, using prototypical neon clusters we have demonstrated that resonant ICD which leads to low-energy electron emission can be detected by measuring the subsequent fluorescence emission. Furthermore, with the help of time resolved measurements the always superimposed signal of atoms and clusters can be perfectly disentangled. Although charged particle detection is a direct proof of ICD, this tool is not available in dense media. On the contrary, fluorescence, as is shown here, provides similar information on interatomic processes and is still applicable to large systems in their natural environment. Moreover, in very dense media, no advanced techniques are required anymore and fluorescence signal is accessible by standard photon-detection schemes as the signal scales with the density. Therefore, first experiments on large clusters and mixed clusters of water and bio-molecules are now possible.

However, future experiments on very dense targets, e.g. liquid jets of water with dissolved biomolecules, will use the combination of selective excitation, dispersed fluorescence and time resolution to discriminate between the many different relaxation pathways available in such a complex system. While the importance of ICD for the generation of low-energy electrons is known, the extreme site selectivity of resonant excitations is just beginning to come to a general consciousness [12]. Combining these properties with a detection scheme which is available in nearly every biology lab, as presented here, will allow a broad scientific community to investigate the details of ionising radiation damage with, hopefully, possible implications to radiation therapy.

Acknowledgements

The work was supported by the State Initiative for the Development of Scientific and Economic Excellence (LOEWE) in the LOEWE-Focus ELCH and by the Deutsche Forschungsgemeinschaft (Forschergruppe FOR 1789 and DFG Project no. DE 2366/1-1). We thank HZB for the allocation of synchrotron radiation beamtime. AIK and LSC acknowledge the financial support from the European Communitys FP7 / ERC AIG No. 227597.

References

[1] Cederbaum L S, Zobeley J and Tarantelli F 1997 *Phys. Rev. Lett.* **79** 4778
[2] Jahnke T *et al* 2010 *Nat. Phys.* **6** 139
[3] Mucke M *et al* 2010 *Nat. Phys.* **6** 143
[4] Hergenhahn U 2012 *Int. J. Radiat. Biol.* **88** 871
[5] Alizadeh E and Sanche L 2012 *Chem. Ref.* **112** 5578
[6] Harbach P H P, Schneider M, Faraji S and Dreuw A 2013 *J. Phys. Chem. Lett.* **4** 943
[7] Hergenhahn U 2011 *J. Electron Spectrosc. Relat. Phenom.* **184** 78
[8] Marburger S, Kugeler O, Hergenhahn U and Möller T 2003 *Phys. Rev. Lett.* **90** 203401
[9] Jahnke T *et al* 2004 *Phys. Rev. Lett.* **93** 163401
[10] Averbukh V *et al* 2011 *J. Electron Spectrosc. Relat. Phenom.* **183** 36
[11] Ottosson N, Faubel M, Bradforth S E, Jungwirth P and Winter B 2010 *J. Electron Spectrosc. Relat. Phenom.* **177** 60
[12] Gokhberg K K, Kolorenč P P, Kuleff A I and Cederbaum L S 2014 *Nature* **505** 661
[13] Trinter F *et al* 2014 *Nature* **505** 664
[14] O'Keeffe P *et al* 2013 *J. Phys. Chem. Lett.* **4** 1797
[15] Kimura M *et al* 2013 *J. Phys. Chem. Lett.* **4** 1838
[16] Kim H-K *et al* 2011 *Proc. Natl Acad. Sci.* **108** 11821
[17] Kim H-K *et al* 2013 *Phys. Rev.* A **88** 042707
[18] Schmoranzer H, Liebel H, Vollweiler F, Müller-Albrecht R, Ehresmann A, Schartner K-H and Zimmermann B 2001 *Nucl. Inst. Methods* A **467–468** 1526
[19] Liebel H *et al* 2000 *Phys. Lett.* A **267** 357
[20] Liebel H, Müller-Albrecht R, Lauer S, Vollweiler F, Ehresmann A and Schmoranzer H 2001 *J. Phys. B: At. Mol. Opt. Phys.* **34** 2581
[21] Liebel H, Ehresmann A, Schmoranzer H, Demekhin P V, Lagutin B M and Sukhorukov V L 2002 *J. Phys. B: At. Mol. Opt. Phys.* **35** 895
[22] Ehresmann A *et al* 2006 *J. Phys. B: At. Mol. Opt. Phys.* **39** L119
[23] Ehresmann A *et al* 2006 *J. Phys. B: At. Mol. Opt. Phys.* **39** 283

[24] Ehresmann A, Kielich W, Werner L, Demekhin P V, Omelyanenko D V, Sukhorukov V L, Schartner K-H and Schmoranzer H 2007 *Eur. Phys. J.* D **45** 235
[25] Demekhin P V 2009 *Phys. Rev.* A **80** 063425
[26] Demekhin P V, Petrov I D, Sukhorukov V L, Kielich W, Knie A, Schmoranzer H and Ehresmann A 2010 *Phys. Rev. Lett.* **104** 243001
[27] Hagena O F 1981 *Surf. Sci.* **106** 101
[28] Aoto T, Ito K, Hikosaka Y, Shigemasa E, Penent F and Lablanquie P 2006 *Phys. Rev. Lett.* **97** 243401
[29] Barth S, Joshi S, Marburger S, Ulrich V, Lindblad A, Öhrwall G, Björneholm O and Hergenhahn U 2005 *J. Chem. Phys.* **122** 241102
[30] Gokhberg K, Averbukh V and Cederbaum L S 2007 *J. Chem. Phys.* **126** 154107
[31] Santra R, Zobeley J and Cederbaum L S 2001 *Phys. Rev.* B **64** 245104
[32] Öhrwall M 2004 *Phys. Rev. Lett.* **93** 173401
[33] Mucke M, Förstel M, Lischke T, Arion T, Bradshaw A W and Hergenhahn U 2012 *Rev. Sci. Instrum.* **83** 063106
[34] Schulz K, Domke M, Püttner R, Gutiérrez A, Kaindl G, Miecznik G and Greene C H 1996 *Phys. Rev.* A **54** 3095
[35] Schartner K-H, Mbus B, Mentzel G, Ehresmann A, Vollweiler F and Schmoranzer H 1992 *Phys. Lett.* A **169** 393
[36] Lablanquie P *et al* 2000 *Phys. Rev. Lett.* **84** 431
[37] Liu W and Dalgarno A 1996 *Astrophys. J.* **462** 502
[38] Kuleff A I and Cederbaum L S 2007 *Phys. Rev. Lett.* **98** 083201
[39] Trinter F *et al* 2013 *Phys. Rev. Lett.* **111** 093401
[40] Schnorr K *et al* 2013 *Phys. Rev. Lett.* **111** 093402
[41] Trinter F *et al* 2013 *Phys. Rev. Lett.* **111** 233004